Hybrid of Eddy Current Probe Based on Permanent Magnet and GMR Sensor

Moneer A Faraj[1], Fahmi Samsuri[1], Ahmed N AbdAlla[2]
[1]*Faculty of Electrical and Electronics, University Malaysia Pahang, Malaysia*
[2]*Faculty of Electronic Information Engineering, Huaiyin Institute of Technology, Huaian, Jiangsu, China*
mod84_91@yahoo.com

***Abstract*—The eddy current testing (ECT) is used to inspect a material to determine its properties without destroying its utility. The applications include detection of flaws in aircrafts, pipeline, etc. An ECT is a weak sensitivity to a subsurface defect. Applications of giant magnetic sensors (GMR) are increasingly applied to the measurement of weak magnetic fields related to the currents they cause. In this paper, GMR sensor with magnet bar (permanent) is utilized. The proposed probe system is utilized to study the impact of the width and depth defect on the signal of eddy current testing. The maximum depth of flaw in a mild steel can be revealed by using this probe. The graph of the difference between the peak amplitude and the penetration depth of each slot of a different width of the two bands of mild steel shows the increase of the signal for each slot and flat above 3mm. The experimental result proves the inability of a PM-GMR probe to detect a defect at a depth of 3mm on a surface defect.**

***Index Terms*—Eddy Current Testing; GMR Sensor; Defect Detection; Non-destructive Testing; Calibration.**

I. INTRODUCTION

The term Eddy Current Testing technique is used widely to assess the condition of the material under test in the oil and gas industry [1, 2]. The measured signal typically contains information conductivity, magnetic permeability or dielectric permittivity[3].

GMR sensors have undergone recent developments to alleviate some of the problems associated with eddy current testing. Due to their superior sensitivity. small dimensions and low cost, these sensors have been proved effective for detection of deeply buried cracks (up to 25 mm below the surface) using eddy current methods. A GMR sensor works together with excitation coils to form the GMR testing probe based eddy current [4, 5].

In this paper A PM-GMR probe using GMR sensor with magnet bar (permanent). This probe system is used for investigating the effect of width and depth of defect on the eddy current testing signal.

II. THEORETICAL BACKGROUND

A. The principle of eddy current testing

In ECT, the excitation coil is excited to generate the variable magnetic field. Based on Faraday's law of electromagnetic induction, it will induce eddy current in the conducting material under test [6-8]. Due to the opposed magnetic field generated by these eddy currents, the pick-up coil, also known as received coils have emf induced in them. The principle diagram of ECT is shown in Figure 1.

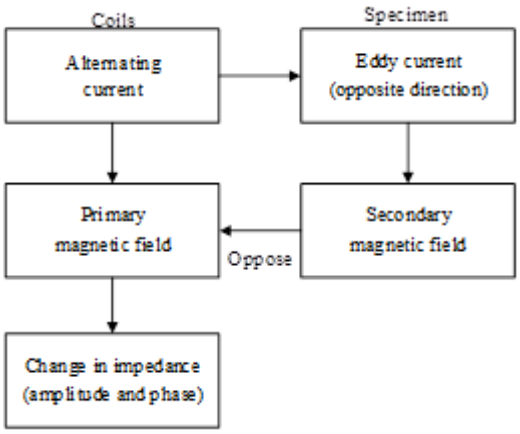

Figure 1: Principle diagram for eddy current testing

Generally, the magnetic field interaction between main and secondary field can be demonstrated based on four steps:

- The coil that carries the alternating current produced the main MF.
- Alternating primary MF causes EC in the conductive sample.
- EC produces secondary MF in opposing direction.
- Flaws in the sample perturb the EC and decrease the secondary MF, which result in the variation of impedance changes of the coil.

The advantages of ECT over other NDT methods are the elimination of physical contact between the probe and the material under test, Low cost, High inspection speed and Environmentally friendly. On the other hand, it is only usable for conductive material and presence of noise due to factors such as probe lift-off and surface roughness [9].

B. Factors Affecting Eddy Current Testing

There are different factors that impact the eddy current testing examination other than the flaws and defects. The signal of an eddy current probe is a combination of responses including the sample geometry, properties of the material and lift-off between the probe and the sample.

1) Frequency

It is one of the important factors to specify the depth of the located defect. Low frequency is utilized to detect a subsurface defect. Furthermore, high frequency is used for the surface defect. Table 1 shows the value of skin depth for a different type of materials at several frequencies [10, 11].

Table 1
Value of Skin Depth for Some Common Materials

Material	1MHz	1KHz	1KHz
Iron	5.03μm	16mm	0.65mm
Wet Soil	0.25m	7.96m	32.5mm
Copper	0.067mm	2.1mm	8.61mm

2) Conductivity and permeability

The magnetic field is affected by the conductivity and permeability, which affects the output of GMR sensor. The electrical conductivity and permeability of test objects of a material, which in turn depends on microstructure, Heat treatment, chemical deposition and hardening temperature [12, 13]. Table 2 summarizes the conductivity of common materials based on the International Annealed Copper Standard (%IACS).

Table 2
Conductivity of Conductive Material

Material	Conductivity (%IACS)
Copper	100.00
Aluminum 2024 T4	32.00
Gold	70.00
Brass	28.00
Stainless steel 316	2.33

3) Lift-off

The distance between the surface of the material and the eddy current probe is defined as the lift-off. The lift-off needs to be fixed and minimized without touching the surface of the material. The magnetic field is ineffective in the case when the lift-off increases, therefore it decreases the probe sensitivity [1, 14].

C. Giant Magneto-Resistance

Investigating deeply cracks and small crack at edges are challenges encountered by the Nondestructive testing (NDT). One of the ways to address this problem is to insert the GMR sensors in eddy current probe. Due to their high sensitivity and small dimension, these sensors have been proved for detection of deeply cracks (up to 25 mm below the surface) using eddy current testing method. [15].

The Giant Magneto-resistive effect (GMR) was discovered in 1988 when a relatively large change of resistance was discovered when compared to AMR materials. When stacked, layers of ferromagnetic and nonmagnetic materials were exposed to a magnetic field [1] as shown in Figure 2.

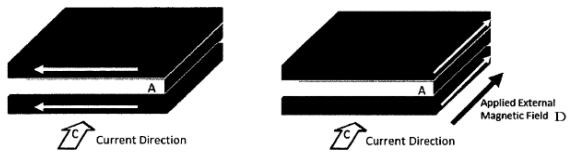

(a) (b)

Figure 2: A diagram illustrating of GMR. a) GMR film layers without an applied magnetic field showing directions of magnetic moments b) GMR layers in the presence of an applied magnetic field

D. Configurations of EC Coil Probes

Common EC probes are designed as a flat coil, pancake coil, or encircling coil [16]. As shown in Figure 3, coil configurations depend on different applications: 1) surface probes (Figure 3(a)) that can be pancaked shaped to scan along the surface and yield magnetic flux perpendicular to the surface; 2) Bobbin (inner diameter) probes (Figure 3(b)) are wound on a bobbin to move along the inside of the tubes and produce axial magnetic flux; 3) Outside diameter probes (Figure 3(c)) that can be wound to encircle the specimen [1, 16].

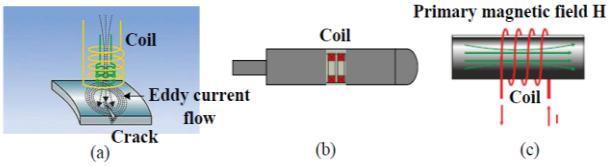

Figure 3: Typical EC probes; (a) Pancake type coil, (b) Bobbin type coil, (c) Encircling type coil.

Coil probes can operate in double-function mode, separate-function mode and hybrid mode. The double-function operation includes two approaches: An absolute probe and a differential. Absolute probes can be overly sensitive to material variations, temperature changes, lift off and other variations during the inspection. Differential probes are relatively insensitive to slow or gradual discontinuity or composition changes of a test structure [2].

Separate-function probes employ a primary coil to provide source currents and a secondary coil (pick-up coil) to sense the secondary field due to eddy currents. Separate-functions probes can also be used in an absolute or differential mode. This probe type is also called Transmit/Receive probe. The configuration of transmit coil is specially designed for optimizing the eddy current flow pattern, and the receiving coil configuration is designed to achieve a maximum sensitivity to defect [17].

III. Material and Method

A. Material

Two blocks of mild steel have been utilized with different dimensions. AutoCAD design software was used to design the artificial defect slots, as shown in Figure 4 and 5. The first block dimension is 250mm length × 50mm width × 10mm height and the second block dimension is 50mm width x 10mm height x 256mm length. The EDM wire cut machine is used to calibrate defect into the surface of mild steel plates. The defect in the first block is from 0.5mm to 4mm slot depth and width 1mm while on the second mild steel block from 1mm to 5mm slot depth and 2 width.

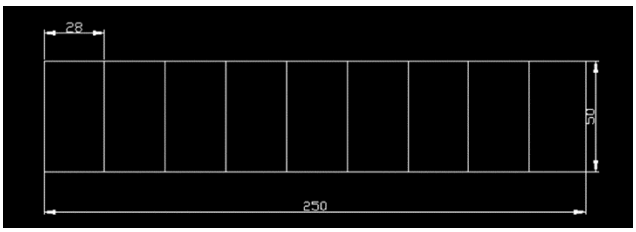

(a)

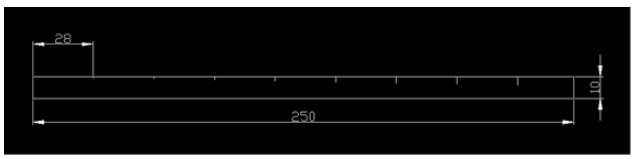

(b)

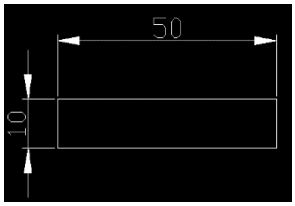

(c)

Figure 4: The first mild steel calibration block; (a) Top view, (b) Side view, (c) Front view.

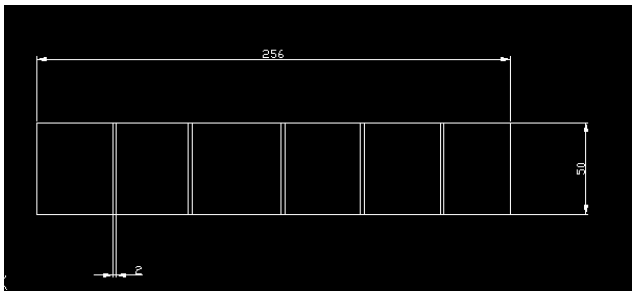

(a)

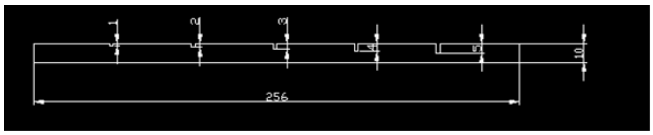

(b)

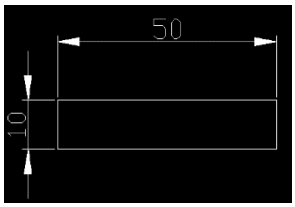

(c)

Figure 5: The second mild steel calibration block; (a) Top view, (b) Side view, (c) Front view.

The proposed hybrid PM-GMR probe technique utilized the excite-pick up mode with a permanent magnet and GMR detection sensor. In order to detect various depth and width of a defect in mild steel plates, the Pro E software is used to design the probe in 3D as shown in Figure 6.

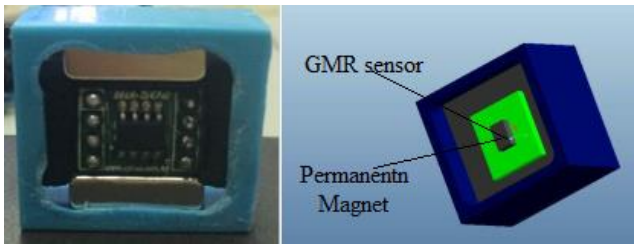

Figure 6: PM-GMR probe; (a) Casing probe Front view, (b) Design the probe using Pro E software.

B. Principle Operation of PM-GMR Probe

The PM-GMR probe is collected of a permanent magnet and NVE AA002-02E GMR sensor as shown in Figure 6 (a). The magnet (Nd2Fe14B) has the dimensions of 20mm length, 15mm width, and 7mm height and is separated from the GMR sensor by a distance of 5mm. The direction of the axis of sensitivity of the GMR sensor is parallel to the surface of the mild steel plate, while the direction of the magnet bar is vertical to it. The component of the magnetic flux generated by the magnet bar is detected by the GMR sensor. When the PM-GMR probe is moved over a mild steel calibration blocks, the output voltage of GMR sensor is constant in the case of no crack. While in the case when the PM-GMR probe is moved over a defect, the magnetization is changed, which alters the result at the peak amplitude of output voltage of GMR sensor.

The 2-D simulation is performed using FEMM. Figure 7 illustrates the contours of the magnetic flux density when the PM-GMR probe moves over a crack of 1mm width and 1mm depth. A uniform magnetization of mild steel plate can be seen in Figure 7(1), (2) and (6). The magnetic flux changes, once the probe approaches a defect as seen in Figure 7(3) and (5). The uniformity of the magnetic flux is changed, when the probe is over the flaw, which is detected by GMR sensor according to high sensitivity as seen in Figure 7(4).

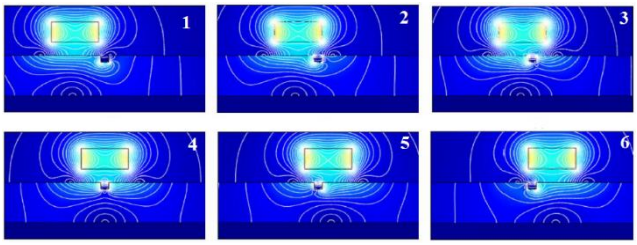

Figure 7: A magnetic model of the MP-GMR probe

When a magnetic bar approaches the mild steel with various width 1mm, 2mm and 2mm depth, the magnetic flux is distributed as in Figure 8.

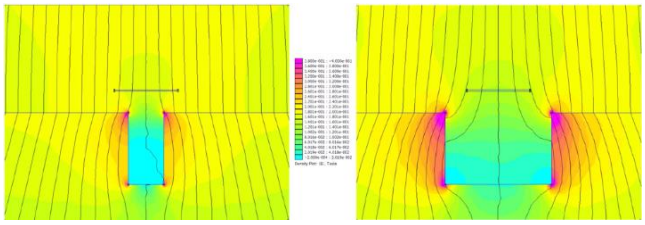

(a) (b)

Figure 8: Magnetic flux lines obtained from 2Dsimulations using FEMM; (a) d=2 mm, w=1mm, (b) d=2 mm, w=2mm.

C. Experimental Setup

The GMR sensor on circuit is connected as the current receiver and a permanent magnet as the current transmitter. Lastly, the complete circuit is connected as shown in Figure 9, then the Arduino and followed with the probe.

Two collections of calibration blocks of mild steel with different dimension have been tested by utilizing the PM-GMR probe. Figure 9 shows an examination of mild steel calibration blocks. All the 8 depth slots with 1mm have been examined. The process is repeated with the second calibration block. All the 5 depth slots with 2mm width have been inspected also.

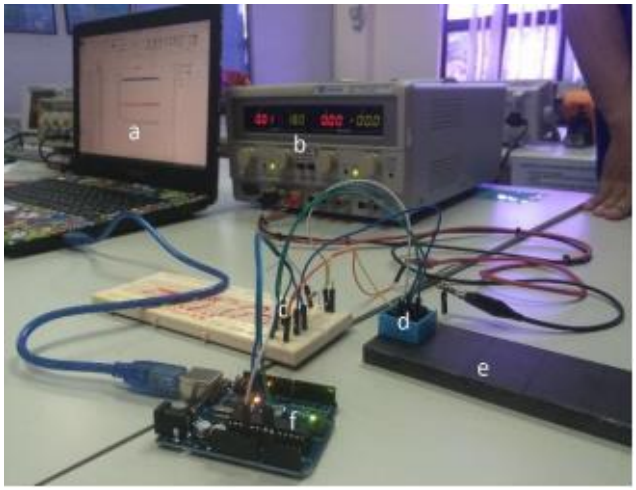

Figure 9: Experimental setup for ECT system for inspection brass calibration block; (a) Monitor, (b) Power supply, (c) Circuit board, (d) PM-GMR probe, (e) Calibration block, (f) Arduino.

IV. Result and Discussion

The first calibration block has been tested, it started from 0.5mm up to 4mm. the outcome signal of the scan PM-GMR probe for 0.5mm is 2.391126V as can be seen in Figure 10.

Figure 10: The first slot in depth of 0.5mm with width 1mm

The inspection of the second calibration block are shown in Figure 11. The peak amplitude voltage of the GMR sensor was obtained from the five crack with depth = 1, 2, 3, 4 and 5 and width = 2mm. The result illustrates that the peak amplitude voltage increases its amplitude proportionally to the depth of defect. However, the value of voltage has a constant amplitude for the depth greater than 3 mm. This is because the penetration of eddy current that was generated by the permanent magnet is 3mm only. This disadvantage can be solved by replacing permanent magnet by excitation coil to increase the depth penetration using low frequency.

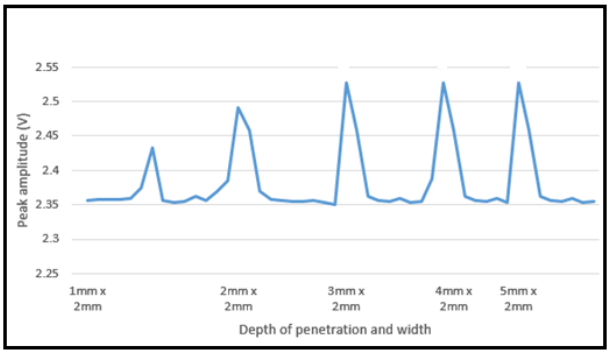

Figure 11: The peak amplitude output voltage of GMR for cracks with d=1, 2, 3, 4 and 5 mm and w= 2 mm

The output voltage signal for all slots of the second mild steel calibration block with depth = 0.5mm, 1, 2, 2.5, 3, 3.5 and 4mm and width= 1mm can be seen in Figure 12.

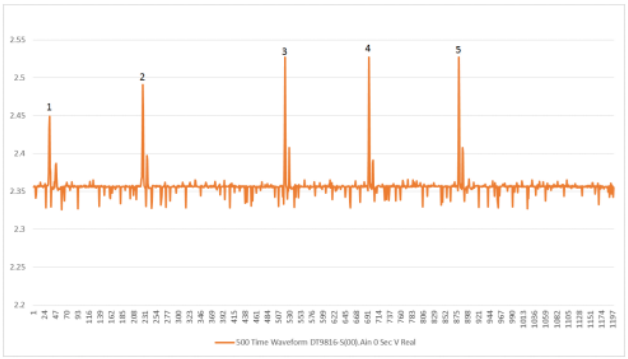

Figure 12: Full scale result for all depth slots of second mild steel block width 2mm

The difference between the peak amplitude and the depth of penetration for each slot of the mild steel is 0.5mm to 4mm. The graph shows the increasing signal for each slot. From the observation, the PM-GMR probe can detect the defect at 3mm depth only, as shown in Figure 13. At 3mm, 3.5mm and 4mm, the reading of the signal is flat.

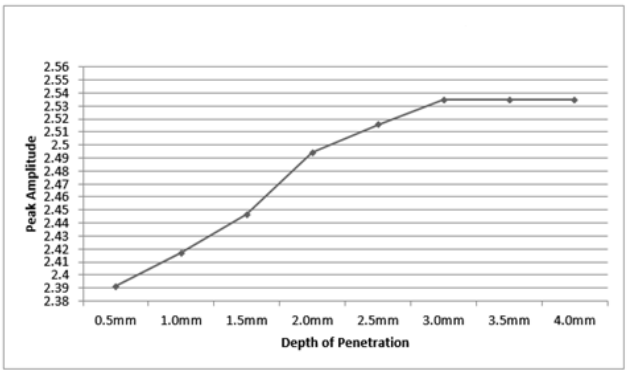

Figure 13: Full reading for signal for all depth slots of mild steel block width 1mm

V. Conclusion

Different factors that impact the penetration of eddy current to examine the subsurface defect such as lift off, conductivity, sensor sensitivity and etc, have been identified. In this paper, the PM-GMR probe for detecting defect with different dimension in mild steel calibration block based on the eddy current technique is presented. The peak amplitude voltage of the GMR sensor is constant above 3mm. This proved that GMR-PM probe operated using a magnetic field can be only detect subsurface at 3mm and less than with the different width. One of the advantages of this probe is that an external source of power for producing the magnetic field is not required.

Future work can be done to increase the depth penetration of the probe to inspect subsurface defect more than 3 mm. This can be done by using an excitation coil and evaluation of subsurface cracks or other excitation frequencies to control the current's depth of penetration.

ACKNOWLEDGMENT

This work was supported by Universiti Malaysia Pahang under project vote RDU1403116

REFERENCES

[1] D. Rifai, A. N. Abdalla, K. Ali, and R. Razali, "Giant Magnetoresistance Sensors: A Review on Structures and Non-Destructive Eddy Current Testing Applications," *Sensors*, vol. 16, p. 298, 2016.

[2] J. García-Martín, J. Gómez-Gil, and E. Vázquez-Sánchez, "Non-destructive techniques based on eddy current testing," *Sensors*, vol. 11, pp. 2525-2565, 2011.

[3] J.-T. Jeng, G.-S. Lee, W.-C. Liao, and C.-L. Shu, "Depth-resolved eddy-current detection with GMR magnetometer," *Journal of Magnetism and Magnetic Materials*, vol. 304, pp. e470-e473, 2006.

[4] K. B. Ali, A. N. Abdalla, D. Rifai, and M. A. Faraj, "Review on system development in eddy current testing and technique for defect classification and characterization," *IET Circuits, Devices & Systems*, 2017.

[5] T. Dogaru and S. T. Smith, "Giant magnetoresistance-based eddy-current sensor," *IEEE Transactions on Magnetics*, vol. 37, pp. 3831-3838, 2001.

[6] C. S. Angani, H. G. Ramos, A. L. Ribeiro, and T. J. Rocha, "Evaluation of transient eddy current oscillations response for thickness measurement of stainless steel plate," *Measurement*, vol. 90, pp. 59-63, 2016.

[7] F. Vacher, F. Alves, and C. Gilles-Pascaud, "Eddy current nondestructive testing with giant magneto-impedance sensor," *NDT & E International*, vol. 40, pp. 439-442, 2007.

[8] D. Rifai, N. Abdalla, N. Khamsah, K. Ali, and R. Ghoni, "Defect Signal Analysis for Nondestructive Testing," *Proceedings of the FluidsChR*, 2015.

[9] C. S. Angani, H. G. Ramos, A. L. Ribeiro, T. J. Rocha, and P. Baskaran, "Lift-Off Point of Intersection Feature in Transient Eddy-Current Oscillations Method to Detect Thickness Variation in Stainless Steel," *IEEE Transactions on Magnetics*, vol. 52, pp. 1-8, 2016.

[10] J. Bowler and M. Johnson, "Pulsed eddy-current response to a conducting half-space," *IEEE Transactions on magnetics*, vol. 33, pp. 2258-2264, 1997.

[11] S. Udpa and P. Moore, "Nondestructive testing handbook: electromagnetic testing," *Amer Society for Nondestructive*, 2004.

[12] J. Xin, N. Lei, L. Udpa, and S. S. Udpa, "Nondestructive inspection using rotating magnetic field eddy-current probe," *IEEE Transactions on Magnetics*, vol. 47, pp. 1070-1073, 2011.

[13] M. A. Faraj, F. Samsuri, A. N. Abdalla, D. Rifai, and K. Ali, "Adaptive Neuro-Fuzzy Inference System Model Based on the Width and Depth of the Defect in an Eddy Current Signal," *Applied Sciences*, vol. 7, p. 668, 2017.

[14] D. Rifai, A. N. Abdalla, R. Razali, K. Ali, and M. A. Faraj, "An Eddy Current Testing Platform System for Pipe Defect Inspection Based on an Optimized Eddy Current Technique Probe Design," *Sensors*, vol. 17, p. 579, 2017.

[15] T. Y. Poon, N. C. F. Tse, and R. W. H. Lau, "Extending the gmr current measurement range with a counteracting magnetic field," *Sensors*, vol. 13, pp. 8042-8059, 2013.

[16] Y.-J. Kim and S.-S. Lee, "Eddy current probes of inclined coils for increased detectability of circumferential cracks in tubing," *NDT & E International*, vol. 49, pp. 77-82, 2012.

[17] R. Ghoni, M. Dollah, A. Sulaiman, and F. M. Ibrahim, "Defect characterization based on eddy current technique: Technical review," *Advances in Mechanical Engineering*, vol. 6, p. 182496, 2014.